Tunnel Lab: Group 2

Natalie Gray, Iman Ebrahimi, and Alex Matilainen
Faculty of Science: Lund University
(Dated: May 10, 2023)

I. INTRODUCTION

Quantum tunneling was first discovered in 1927 by Friedrich Hund while observing the double well potential. Tunneling is a process where quantum particles have a certain probability, which is determined by the wave function, to pass through a potential barrier and appear on the other side. It is similar to the effect of light and a piece of glass. Some of the incoming light will be reflected off the glass, while the rest will be refracted. Instead of being determined by an index of refraction, however, it is determined by the coefficient of transmission, which is derived from case-specific solutions to the Schrödinger equation. The transmission coefficient is reliant on the energy of the particle, the strength of the potential, and most importantly, for this lab, the width of the potential barrier. The goal of this exercise is to use electrons and quantum tunneling to determine four numerical values from four different potential barrier setups. The experiment consists of two different single potential barriers where the width of the barrier will be measured and two different double potential barriers where the distance between the two barriers will be experimentally determined. These measurements are accomplished by arranging a circuit so electrons can be fired toward a potential barrier. Some of those electrons are emitted where they subsequently reach a drain and complete the circuit, which also measures the output.

II. THEORETICAL BACKGROUND

A. Single Potential Barrier

The single potential step problem is composed of one material, of a higher potential, sandwiched in between a different material which creates the barrier shown in Figure 4.

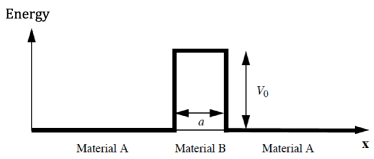

FIG. 1: The figure shows the layout for the experimental setup consisting of the two materials of different potentials with the barrier $V_0 = 200meV$. The graph shows energy as a function of position x, with a being the width of the potential barrier [1].

The initial conditions of the system must be understood to theoretically determine the width of the barrier. A particle is incoming from the left at energy, E, which is less than V_0. The particle can either be reflected or transmitted through the barrier. The probability of reflection and transmission added together must equal 1. Once inside the barrier, the particles will encounter this probability again and will either be reflected or transmitted through the other side of the potential step. Finding these probabilities is done by solving the time-independent Schrödinger Equation, which is given by,

$$E\phi(x) = \frac{-\hbar^2}{2m}\frac{d^2\phi(x)}{dx^2} + V(x)\phi(x). \tag{1}$$

This equation is solved in three regions: Material A on the left-hand side, Material B, and Material A on the right-hand side. The solution produces five different coefficients A_I the incoming particle, B_I the reflected particle, A_{II} the transmitted particle inside the barrier, B_{II} the reflected particle inside the barrier, and A_{III} the fully transmitted particle. These coefficients provide the tools to find the transmission coefficient. The transmission coefficient needs to be measured in order to experimentally determine the width of the barrier and it is given by the equation,

$$T(E) = \left|\frac{A_{III}}{A_I}\right|^2. \tag{2}$$

After determining the solutions to the Schrödinger Equation and the subsequent coefficients, the transmission coefficient is given by,

$$T(E) = e^{-2ka}, \tag{3}$$

where

$$k = \sqrt{\frac{2m}{\hbar^2}(V_0 - E)}. \tag{4}$$

In these equations, a is the width of the barrier and m is the mass of the particle. Experimentally, however, these equations are slightly altered due to an applied bias to the circuit. The new form of the barrier is described by Figure 2.

This new potential barrier design, however, can be approximated to a barrier of smaller height,

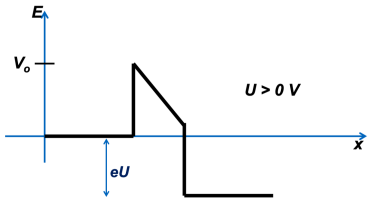

FIG. 2: The figure shows the layout for the experimental setup, but now with an applied bias to the circuit [1].

$$V = V_0 - e\gamma\frac{U}{2}, \tag{5}$$

where γ is a scaling factor of the value 0.3 for the devices used in the experiment and U is the introduced bias.

The final equation for the transmission coefficient for the single barrier experiment and the one used in further calculations is given by,

$$T(E) = e^{-2a\sqrt{\frac{2m}{\hbar^2}(V_0 - e\gamma\frac{U}{2} - E)}}, \tag{6}$$

after substitutions are made for V and k, the value for E is the energy of the electron, which is 0, when close to the band bottom due to the cooling mechanism introduced in the experiment.

B. Double Potential Barrier

The double potential step follows a very similar approach only now the setup is shown in the graph in Figure 3.

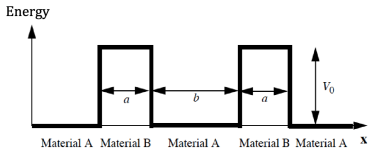

FIG. 3: The figure shows the layout for the experimental setup consisting of the two materials of different potentials with the barrier $V_0 = 200meV$. The graph shows energy as a function of position x, with a being the width of the potential barrier and b being the width between the two barriers.

The double potential barrier also requires the solutions to Equation 1, but in this case, will have 9 coefficients to find solutions for. The transmission coefficient in this case is given by

$$T(E) = \frac{T_B^2}{T_B^2 + 2(1 - cos(2kb))}, \tag{7}$$

where

$$k = \sqrt{\frac{2mE}{\hbar^2}}. \tag{8}$$

T_B is the approximated transmission through each barrier and E has resonances defined by the equation,

$$E = \frac{\gamma eU}{2} = \frac{\hbar^2\pi^2n^2}{2mb^2}. \tag{9}$$

The part of the equation, $(\gamma eU)/2$, came from the same reasoning seen in the single potential barrier where a bias was applied and the new potential was estimated at a fraction of the height of the bias. The width of the barrier directly affects the location of resonances in the bias. In the second part of the equation, the energy is represented by different states, n, where $n = 1, 2, 3, ...$ and b is the width between the two potential barriers. The equation is similar to the bound states in an infinite potential well, which the experimental setup resembles. In between the two barriers, the particles will behave similarly to the infinite potential system, by creating different energy resonances. By connecting the two equations through energy, the bias now redefines the ground state and creates an exponential curve with resonances sprinkled throughout.

III. METHODS

This experiment used four different samples each with a varied potential barrier setup. The device's electrical system used for this experiment is placed inside a container filled with liquid nitrogen for the entirety of the trial. This procedure increases the accuracy of obtaining the necessary data since it typically heightens the likelihood of tunneling occurrences. We proceeded with the experiment by connecting the mechanism to a computer, which enabled us to manage the input voltage, track the output current, and visualize the data using simulation software. The schematics of the mentioned system are shown in Figure 4

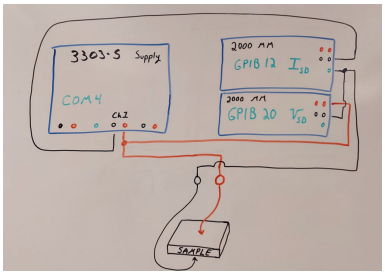

FIG. 4: The figure shows a schematic diagram of the layout for the experimental setup including the source unit, the sample in liquid Nitrogen, and measurement devices to track the current and voltage. [2]

Starting at 0 volts, we gradually raised the voltage while carefully tracking the behavior of the output current. The voltage was incrementally raised up to 1 volt, and the change in current for each sample was studied. Throughout the experiment, four separate configurations were running concurrently. That is, one single-barrier circuit, two double-barrier circuits, and a fourth sample which resulted in a statistical anomaly due to its technical defects. Each configuration was rotated between the groups to take measurements. After each trial, the data was saved as a .txt file and the numerical analysis was conducted using Excel.

IV. RESULTS

A. Single Potential Barrier

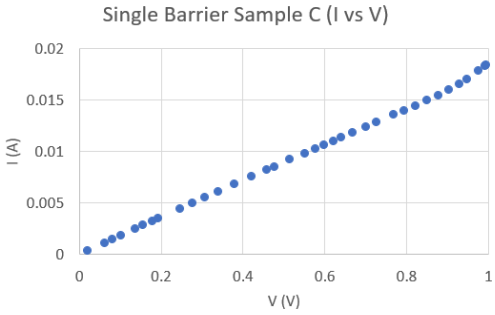

FIG. 5: The figure above displays the results of undergoing the procedure on the Broken Single Barrier Sample C. The y-axis is the current value measures in Amperes and the x-axis is the voltage value measured in Volts.

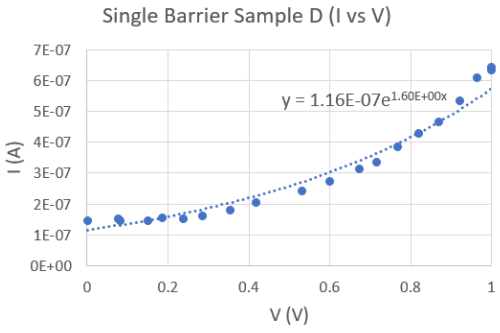

FIG. 6: The figure above displays the results of undergoing the procedure on the Single Barrier Sample D. The y-axis is the current value measures in Amperes and the x-axis is the voltage value measured in Volts. The exponential equation of best fit is also shown on the graph.

Only one of the single barrier samples provided adequate data, with Sample C being broken and producing a straight line where an exponential curve should be. The exponential curve was utilized to find the value of the barrier width a.

B. Double Potential Barrier

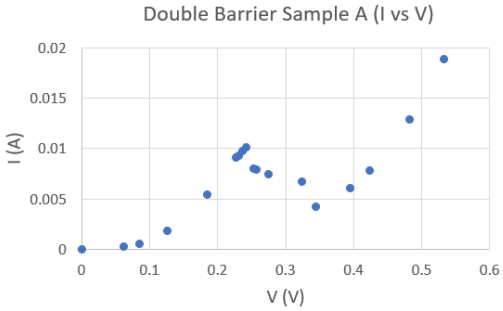

FIG. 7: The figure above displays the results of undergoing the procedure on the Double Barrier Sample A. The y-axis is the current value measures in Amperes and the x-axis is the voltage value measured in Volts.

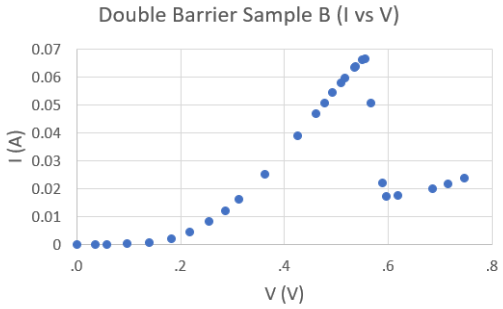

FIG. 8: The figure above displays the results of undergoing the procedure on the Double Barrier Sample B. The y-axis is the current value measures in Amperes and the x-axis is the voltage value measured in Volts.

Both of the double barrier samples were in working condition and provided adequate results, producing a noticeable peak that allowed us to calculate the barrier width value b for both samples.

V. ANALYSIS

A. Single Potential Barrier

In order to calculate the barrier width a, Equation 6 was utilized to demonstrate a relationship between the current I and the voltage V. The transmission coefficient $T(E)$ is given as proportional to the current I, so $T(E) \propto I$. This relationship allows for mathematical analysis to be performed on Equation 6 to develop a linear relationship where the slope is proportional to the width value a.

Firstly, the two sides of relationship $T(E) \propto I$ have the natural log applied to them to remove the e factor in Equation 6, resulting in the equation

$$\ln(I) = \ln(A) - 2a\sqrt{\frac{2m}{\hbar^2}}\sqrt{(V_0 - e\gamma\frac{U}{2})}\,, \qquad (10)$$

where A is a constant of proportionality that can be ignored for the purposes of this analysis. This equation then represents a linear dependency between $\ln(I)$ and U where a is equal to the negative slope.

This dependency was then graphed using the data from Sample D to provide a value for a found from the negative slope when graphing the relationship described in Equation 10. The graph can be seen in Figure 9.

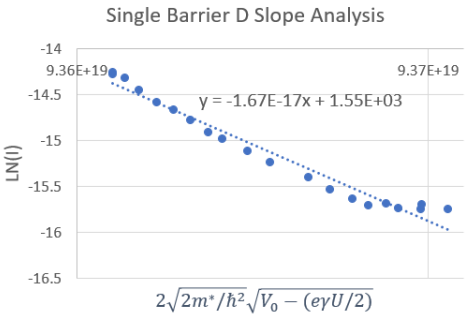

FIG. 9: The figure above displays the linear relationship as described in Equation 10. The slope is equal to $-a$, where the y-axis is equal to the left-hand side of the equation while the x-axis is equal to the right-hand side, where the constant of proportionality, A, is disregarded.

This process was only able to be done on Sample D because Sample C was broken and did not provide results worthy of analyzation.

B. Double Potential Barrier

In order to calculate the barrier width b for the double barrier samples utilizing the voltage values Equation 9 is used. In order to utilize the equation however, the first resonance is considered where $n = 1$, and the energy is then zeroed, resulting in the relationship shown in Equation 9.

This process is similar to what is done in the single barrier samples as seen in Equation 5. This relationship is then applied to the peak values of the current in Figures 7 and 8. The voltage values utilized are $2.42 * 10^{-1}\,V$ and $5.55 * 10^{-1}\,V$ respectively. These U values are then applied to Equation 9 along with the values $\gamma = 0.3$, $n = 1$, and $m = 0.067\,m_e$ to calculate the values for b.

After undergoing the necessary calculations, the b value for Sample A was found to be $12.4\,nm$ while the value for Sample B was found to be $8.21\,nm$.

VI. DISCUSSION

With regard to both experiments, the exponential I-U curve depicted in Figure 6 conforms to the theoretical prediction, while the corresponding curve in Figure 5, for the broken sample, appears completely linear. Furthermore, Figure 7 and Figure 8 present a peak in the I-U curve (the first resonance) that is also in agreement with the theoretical prediction. We observe that the I-U curve in Figure 9 is not entirely linear. Nonetheless, the curve would approximately follow a linear trend for the studied values and therefore conforms to the predicted behavior.

Considering the single-barrier setting, When the negative of the slope is used to calculate a, the value is found to be $1.67 * 10^{-8}\,nm$. This value is eight orders of magnitude off from the expected range of $10\,nm$, so there must be something wrong with the methods used for analysis seeing that the data appears to be adequate.

Further considerations of theory and experiment would remind us of the fact that in a double-barrier setting, a theoretical infinite well is anticipated to have various bound excited states, each of which would be observable on an extended graph as successive resonance peaks. This appears to be somewhat contrary to the case when observations are made in a practical setting, and the depth of the potential well plays an essential role. Particularly in the case of this experiment, the potential well is deep enough for only one such bound state. If the electron's energy were at the level of the first excited state (That is, $n = 2$), the potential would thus be higher than the first potential barrier, preventing any tunneling occurrences. Therefore, only one peak is observed when considering the I-U graph.

As stated, the objective was to calculate the barrier width value for each of the setups. By performing the necessary measurements, we were able to determine that the b value for Sample A was found to be $12.4\,nm$ while the value for Sample B was found to be $8.21\,nm$. The results were in reasonable agreement with theoretical predictions, leading us to conclude that this experiment was successfully conducted and the results were to our satisfaction.

VII. ACKNOWLEDGMENTS

All three group members set up and performed the experiment. Natalie wrote the introduction and theoretical background; Alex wrote the results and analysis; Iman wrote the methods and discussion.

[1] Lab Manual Tunnel Lab
https://canvas.education.lu.se/courses/22074/files/3655940?module_item_id=865815

[2] Tunnel Lab Powerpoint files/3659935?module_item_id=866476
https://canvas.education.lu.se/courses/22074/